



Virial Theorem and Scaling Analysis in Infinitely Confined Quantum Dots

Celalettin Demir ^{1,a,*}

¹ Physics Department, Karaman Science and Art Center, Ministry of National Education, Karaman, Türkiye.

*Corresponding author e-mail address: celdemir70@gmail.com

Research Article

History

Received: 04.01.2026

Accepted: 12.03.2026



This article is licensed under a Creative Commons Attribution-NonCommercial 4.0 International License (CC BY-NC 4.0)

ABSTRACT

The virial theorem is a fundamental principle giving the relationship between kinetic and potential energies in classical and quantum mechanical systems. In this study, the virial theorem was investigated using the scaling method in quantum dot structures. Two different approaches were used; the wave function of the position vector was scaled only in the first approach, while the dot radius was scaled only in the second approach. This method is valid not only for single-electron systems but can also be applied to multi-electron systems. In the calculations, the virial theorem was satisfied. Furthermore, the average energy of the system was minimized, and so on demonstrating that this approach provides a highly accurate and stable framework for multi-electron systems.

Keywords: Energy optimization, Quantum dots, Scaling, Virial theorem.

^a 0000-0002-0393-5931

1. Introduction

The virial theorem which clarified the relationship between kinetic and potential energies in physical systems was first formulated by Clausius in the 1870. Clausius defined the term 'virial' as the mean of the product of position coordinates and forces in the system and showed that its magnitude is equal to the average kinetic energy of the system, but opposite in sign [1]. In the last century, the virial theorem has been successfully applied to the solution of physical problems in many different fields such as astrophysics, cosmology, molecular physics, quantum mechanics and statistical mechanics [2-5].

Studies conducted in the early 20th century established the theoretical background that enabled the formulation of the quantum virial theorem in subsequent years [6-7]. Finkelstein, expanding the theoretical basis, first clearly formulated the quantum virial theorem in the context of Schrödinger wave mechanics. He made the virial theorem applicable to quantum systems by deriving the relationship between the average kinetic and potential energies of the system directly from the wave function [8].

Fock generalized the virial theorem to quantum systems by combining the variational principle and the scaling method. His result showed that virial theorem is valid not only for exact solutions but also for approximate solutions. Hence, derivative of energy terms goes to zero guarantee the virial theorem if a scale parameter is applied to the wave function [9].

Slater, who expanded Fock's framework, applied the virial theorem to a molecule by assuming the nuclei were

kept fixed by external forces. Slater's work has enabled the extension of the virial theorem from atomic to molecular systems [10]. Hirschfelder expanded Fock's approach to problems involving metals and molecules in which the distance between the nuclei is used as a parameter [11]. Another important milestone, contributing directly to the theory of molecular bonding, was achieved by Coulson and Bell. These researchers generalized Hirschfelder's method based on the scaling of the wave function to molecular systems where the internuclear distance is an independent variable [12]. Löwdin treated this subject more systematically. In his work, Löwdin discussed the virial theorem by scaling not only the electron coordinates but also the internuclear distances. He emphasized that the virial theorem is a necessary but not sufficient condition for measuring the accuracy of wave functions [13]. Argyres derived a general virial theorem for systems consisting of interacting particles, where external forces and boundary conditions apply [14].

Classic virial theorem is not directly valid because of contributions and discontinuity of potential energy in confined quantum systems. Potential energy function usually shows discontinuity in systems with a sectional potential structure. Even if the wave function itself remains continuous, its derivative behaves discontinuously at the boundary. In this case, surface integrals emerging during the derivation of the virial theorem introduce additional contributions. Therefore, the virial theorem for systems with sectional potentials must be reformulated in a generalized form that explicitly

includes potential discontinuities and surface effects arising from boundary conditions.

Based on this theoretical framework, Fernández and Castro have conducted several studies to reformulate the virial theorem in confined systems. In these studies, the virial theorem associated with variational methods for systems confined by potential discontinuity and scaling procedure was developed. In this way, a valid form of the virial theorem in quantum dot structures was derived [15-18]. Later, the same authors demonstrated that the virial theorem remains valid in quantum dot structures in case of using approximate wave functions [19]. Katriel and Montgomery redefined the virial theorem for the systems with sloped and smooth sectional potentials by extending Fernández's approach [20]. Mukhopadhyay and Bhattacharyya obtained results for the virial theorem that are consistent with semi-classical methods [21]. Mukherjee emphasized that the classical virial form is generally not valid in the confined systems [22].

Cabrera-Trujillo and Vendrell indicated that the zero wave function condition at the boundary creates a "hidden force" effect by reconsidering the virial theorem for infinite potential boxes in the context of Cauchy boundary conditions [23]. Sezer utilized the virial theorem not only as a physical equation but also as a parameter for error checking [24]. Demir et al. calculated virial coefficients for helium and lithium trapped in infinite spherical potentials. In their work, the virial coefficients were calculated by using wave functions constructed from linear combinations of Slater-type orbitals (STO) [25].

In this study, the energy minimization has been carried out for multi-electron quantum dot structure systems confined by an infinite potential barrier by using the Hartree-Fock-Roothaan (HFR) method together with the Quantum Genetic Algorithm (QGA) method. The scaling process was performed without violating the boundary, normalization, and orthogonalization conditions of the wave function. Unlike similar approaches in the literature, the virial theorem is directly applied to quantum dot structures with sharp boundary conditions, demonstrating that it can be consistently satisfied in these systems. Moreover, proposed method is generalized to multi-electron quantum dot structures. This work distinguishes itself from the existing literature by incorporating the virial theorem not merely as a consistency test, but as an integral part of the HFR-QGA-based energy optimization in multi-electron systems. In this respect, the present study offers a new methodological approach to the literature by expanding the traditional use of the virial theorem in quantum dot structure modelling.

2. Materials and Methods

Time independent Schrödinger equation of a multi-electron system is given by:

$$\hat{H} \Psi = E \Psi \tag{1}$$

Here, \hat{H} represents the Hamiltonian operator, E is the total energy of the system, and Ψ denotes the multi-electron total wave function. For spherically symmetric quantum dot structures, this total wave function is constructed as a Slater determinant (or a linear

combination of determinants) consisting of one-electron wave functions. In spherically symmetric systems, single-electron wave function can be divided into its components as;

$$\psi_i(r_i) = R_{n_i l_i}(r_i, a) Y_{l_i m_i}(\Omega_i) \chi_{s_i}(\sigma_i) \tag{2}$$

Here a represents the radius of the quantum dot structure, $R_{n_i l_i}(r_i, a)$ is the radial wave function, $Y_{l_i m_i}(\Omega_i)$ denotes the spherical harmonics, and $\chi_{s_i}(\sigma_i)$ is the spin function. Radial wave functions are constructed from a linear combination of Slater type basis functions (STO):

$$R_{n_i l_i}(r_i, a) = \sum_{\tau=1}^{\sigma_i} c_{\tau i}(a) r_i^{n_i-1} e^{-\zeta_{\tau i} r_i} \tag{3}$$

Here the expansion coefficients ($c_{\tau i}$) and the exponential parameters ($\zeta_{\tau i}$) are treated as variational parameters during variational optimization. For the quantum dot structure system with confined N electrons, general form of the Hamiltonian operator is written below:

$$\hat{H} = - \sum_{i=1}^N \frac{1}{2} \nabla_i^2 - \sum_{i=1}^N \frac{Z}{r_i} + \sum_{i=1}^N \sum_{i < j}^N \frac{1}{r_{ij}} + V_{conf}(r) \tag{4}$$

In this expression, ∇_i^2 represents the Laplacian operator corresponding to the kinetic energy of the i th electron, $\frac{Z}{r_i}$ is the nuclear-electron potential, $\frac{1}{r_{ij}}$ denotes the electron-electron interaction, and $V_{conf}(r)$ is the confinement potential.

Confining potential for a quantum dot structure confined by an infinite spherical potential barrier is defined as:

$$V_{conf}(r) = \begin{cases} 0, & r < a \\ \infty, & r \geq a \end{cases} \tag{5}$$

The value to be minimized with variational optimization is the average energy. For multi-electron systems, average energy is written as the sum of the average of kinetic, nuclear potential, Coulomb and exchange energies:

$$E_{av} = \sum_i \langle i | -\frac{1}{2} \nabla^2 | i \rangle_{av} + \sum_i \langle i | -\frac{Z}{r_i} | i \rangle_{av} + \sum_{i > j} \sum_j \left[\langle ij | \frac{1}{r_{12}} | ij \rangle_{av} - \langle ij | \frac{1}{r_{12}} | ji \rangle_{av} \right] \tag{6}$$

Here i and j represent the orbital indices. If this expression is minimized by variational methods, the approximate form of the wave function that gives the

lowest energy is obtained. However, energy minimization is not enough for physical accuracy. Therefore, the wave function must satisfy the virial theorem as an additional consistency condition.

Virial theorem gives the relationship between average kinetic energy and potential energy in a bound quantum system whose Hamiltonian is $\hat{H} = \hat{T} + \hat{V}$ [26].

$$2T = \sum_i r_i \nabla_i V(r_i) \tag{7}$$

Here, T and V denote the expectation values of the kinetic and potential energy operators. If potential energy $V(r_i)$ is homogeneous of degree n virial theorem is given as:

$$2T = -nV \tag{8}$$

Classical form of the virial theorem in the case of atoms and molecules where $n=1$ for potential energy

$$2T = -V \tag{9}$$

is obtained.

2.1 Variational Optimization

The systems examined in this study are hydrogen-like quantum dot structure with impurity at its center ($Z=1$) and represented by $1s^1$ configuration and helium-like quantum dot structures with impurity at its center ($Z=2$) and $1s^1 2s^1$ configuration. Both systems are confined with infinite potential under spherical symmetry and radial behavior of the wave function was defined under this boundary condition. In the study, principal quantum number was always taken as $n=1$ in all basis functions for hydrogen-like quantum dot structure. A single common basis set was used for both orbitals ($1s$ and $2s$) in the helium-like multi-electron system. However, in order to increase the variational flexibility of the basis functions, principal quantum numbers of basis functions were selected as a combination of both $n = 1$ and $n = 2$ values. Furthermore, a penalty function within the algorithm that enforces the number of nodes of the $1s$ orbital to be zero and the number of nodes of the $2s$ orbital to be one was used for preventing the variational search space from drifting towards non-physical solutions.

During the creation of initial wave functions, a starting population was generated consisting of one hundred individuals by randomly selecting radial expansion coefficients (c_i) and orbital exponential parameters (ζ_i). Five ($\sigma=5$) and seven ($\sigma=7$) basis functions were used for each orbital in hydrogen-like and helium-like systems, respectively. Preferring a wider basis set for helium is due to more complex correlation effects than hydrogenic systems.

After each individual in the population is created boundary, normalization and orthogonalization conditions were provided directly via expansion coefficients. Ensuring the orthogonality condition was utilized via the Gram–Schmidt method. Thus, every individual in the population is guaranteed to produce a physically acceptable initial wave function. In the variational optimization process, Hartree–Fock (HF) and

Quantum Genetic Algorithm methods were used together. Genetic operations, including selection, crossover, and mutation, were carried out in accordance with the algorithm scheme suggested in the study of Çakır et al [27]. The number of iterations was determined as 15000 because this iteration number is value where the average energy reaches a stable plateau region. Therefore, optimized population composed of individuals who are energetically stable and physically consistent was transferred to the scaling step.

Since the scaling process is computationally expensive, the variational optimization was completed first. Subsequently, the same HF+QGA framework was retained during the scaling approach. The scaling approach was applied exclusively to individuals that are physically consistent, meet boundary, normalization and orthogonality conditions, and are optimized in terms of energy. In this way, the computational cost is reduced and the convergence stability of the process is strengthened.

2.2 Virial Scaling Approach

Due to the discontinuity of the potential energy at $r=a$ in quantum dots confined by an infinite potential, the direct application of the classical virial theorem is impossible. For this reason, Fernández and Castro obtained a virial relation valid for full wave functions, which includes the contribution at the boundary surface [16].

$$[\hat{H}, \hat{\nu}] = \frac{a^3}{2} \left(\frac{dR_{n,l}}{dr} \Big|_{r=a} \right)^2 \tag{10}$$

Here $\hat{\nu}$ is an operator defined in the form $r \frac{\partial}{\partial r}$.

Eq. (10) is valid only for complete solutions and needs to be converted so that it can be used with approximate wave functions. In this study, a two-step scaling procedure was developed to apply the virial relation to approximate functions.

i. Position Scaling

Only the position vector is scaled, the radius parameter is fixed. This transformation introduces a new parameter to the wave function:

$$\psi_i^{(\eta r)}(r_i, a) = \eta^{\frac{3}{2}} \psi_i(\eta r_i, a) \tag{11}$$

Here η is the scaling factor.

ii. Radius Scaling: Physical Scaling

Only the radius of the system is scaled:

$$\psi_i^{(\eta a)}(r_i, a) = \psi_i(r_i, \eta a) \tag{12}$$

The boundary, orthogonality, and normalization conditions break down because the scaling process completely alters the physical shape of the wave functions. If these conditions are re-satisfied for the functions with a scaled radius, they will be automatically met for the position-scaled function as well. Moreover, the energy components of the system are calculated

through the auxiliary function and the average energy of the system is given as:

$$E(\eta, a) = \eta^2 T(1, \eta a) + \eta V(1, \eta a) \tag{13}$$

If the derivative of Eq. (13) is taken with respect to the scale parameter,

$$2\eta^2 T(1, \eta a) + \eta V(1, \eta a) + \eta^3 \frac{d}{d\eta} T(1, \eta a) + \eta^2 \frac{d}{d\eta} V(1, \eta a) = 0 \tag{14}$$

equality is obtained. If Eq. (14) is rearranged, the following virial relation is obtained:

$$2T(\eta, a) + V(\eta, a) + a \frac{dE(\eta, a)}{da} = 0 \tag{15}$$

This result is consistent with the virial form given by Fernández–Castro for approximate wave functions [19].

After the mathematical structure of the scaling method is established, the scale parameter (η) must be determined to provide the physical stability point for each individual. In order to find the scale parameter (η) value for each individual, Eq. (14) was solved numerically by the bisection method. Thus, η ensuring virial compatibility was obtained for each individual. At the end of this process, the average energy given in Eq. (13) was recalculated based on the radius-scale wave function of each individual. These newly energy values obtained were used as an equivalent measure to variational energy minimization and optimized population was updated using the HF + QGA procedure applied in the previous section again for 10 iterations.

Finally, the calculated η coefficient was combined with parameters c_i and ζ_i without altering the wave function's functional form:

$$c'_i = \eta^3 \eta^{n_i-1} c_i, \quad \zeta'_i = \eta \zeta_i \tag{16}$$

Thus, for every a energy-minimized and optimized wave functions that satisfy the virial theorem were obtained.

3. Results and Discussion

In this study, approximate wave functions were achieved for hydrogen-like (H 1s¹) and helium-like (He1s¹2s¹) spherical quantum dot structures containing impurities in the center using variational optimization and scaling based virial approach.

As a quantitative measure of the virial deviation,

$$\Delta_{virial}(a) = 2T(\eta, a) + V(\eta, a) + a \frac{dE(\eta, a)}{da} \tag{17}$$

The virial deviation was calculated for each radius and was expected to converge to zero in the ideal case. The results strongly confirm the expected behavior for both H1s¹ and He1s¹2s¹. It is seen that the magnitude of the virial deviation remains on the order of 10⁻⁸ throughout the entire radius range as shown in Table 1. These results show that when the scaling approach is used together with variationally optimized wave functions, the virial theorem is satisfied with extremely high accuracy.

Table 1. Virial residuals for the confined H 1s¹ and He 1s¹2s¹ systems

a	$\Delta_{virial}^{H1s^1}$	$\Delta_{virial}^{He1s^1 2s^1}$
0.5	-3.81×10 ⁻⁸	4.78×10 ⁻⁸
1	8.69×10 ⁻⁹	-4.51×10 ⁻⁸
2	-2.93×10 ⁻⁸	3.32×10 ⁻⁸
3	2.56×10 ⁻⁸	-2.06×10 ⁻⁹
4	2.16×10 ⁻⁸	-1.91×10 ⁻⁹
5	6.88×10 ⁻⁹	2.27×10 ⁻⁸
10	8.27×10 ⁻⁹	-4.18×10 ⁻⁸

The average energy was calculated for hydrogen-like (H1s¹) and helium-like (He1s¹2s¹) quantum dot structures, comparing cases with and without the application of scaling (Table 2). After the scaling process, the average energy showed only very small changes. Especially in the hydrogen-like one-electron system, average energy values are almost the same as illustrated in Table 2. This result shows that the virial theorem affects the distribution of kinetic and potential energies rather than the total energy.

Table 2. Average configuration energies before and after scaling, and scaling parameters as a function of radius.

a	η_{H1s^1}	E_{H1s^1} (Unscaled)	E_{H1s^1} (Scaled)	$\eta_{He1s^1 2s^1}$	$E_{He1s^1 2s^1}$ (Unscaled)	$E_{He1s^1 2s^1}$ (Scaled)
0.5	1.002688	14.749740	14.749696	1.000208	79.391418	79.391331
0.6	0.999728	9.528049	9.528046	0.999911	52.263130	52.263127
0.8	1.000341	4.543545	4.543543	0.960321	26.277091	26.258533
1	0.999831	2.374171	2.374171	1.009911	14.523340	14.551456
1.4	1.000050	0.647114	0.647114	1.004744	5.106109	5.105776
3	1.000230	-0.423967	-0.423967	0.996066	-1.332637	-1.332699
5	0.999977	-0.496410	-0.496410	0.995301	-2.030726	-2.030742
10	0.999983	-0.499999	-0.499999	0.998509	-2.165061	-2.165065

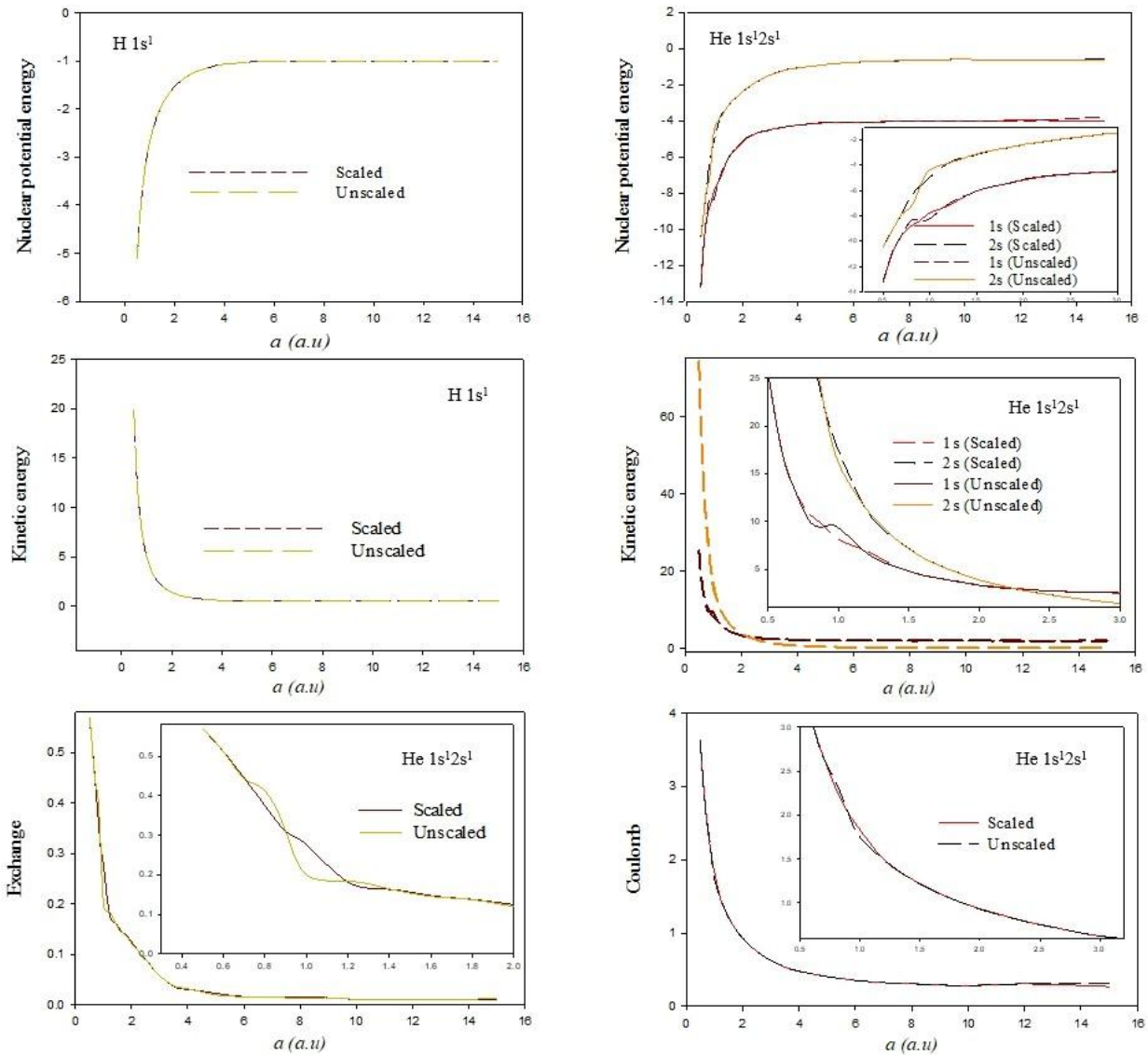


Figure 1. Radius-dependent change of energy expressions of one-electron and two-quantum dot structures (H 1s¹ and He 1s¹2s¹) confined by an infinite potential barrier

When the energy components are examined one by one, the analysis offers a more detailed view (Figure 1). In the hydrogen-like system, the scaled and unscaled energy curves overlap perfectly. This harmony arises from the simple physical structure of the one-electron system. In contrast, the difference between the energy components in the helium-like two-electron system is more pronounced. Due to the presence of two-electron correlation effects and the necessity of preserving the node structure, this distinction may be attributed to variational optimization remaining at a point further from the virial balance before scaling.

The variations of the virial coefficients, defined as the potential-to-kinetic energy ratio (V/T), as a function of radius are illustrated in Figure 2. As expected, as the radius of the dot structure increases, this ratio approaches -2 , and the scaling process leads to a visible improvement in the corresponding curve for the He 1s¹2s¹ system. The results obtained with approximate wave functions are compared with the surface-derivative-based virial expression formally derived from the Schrödinger

equation. The formally exact expression in Eq. 10 and the scaled virial form in Eq. 15 were analyzed together. The corresponding derivative terms were compared as functions of the radius, as shown in Figure 3. Thus, the consistency of both the surface derivative behavior and the energy-based derivative virial term in confined systems was thoroughly tested. For the H 1s¹ system, the profiles of these two terms coincide almost perfectly as a function of the radius. Any observed differences remain within the limits of numerical precision. This shows that the basis functions used in the one-electron system represent both the boundary condition and the surface-derivative behavior very successfully.

For the He1s¹2s¹ system, significant differences emerge between the two quantities (Figure 3). It is observed that as the radius increases, the boundary effect diminishes. Consequently, the energy terms converge and the discrepancy between the two approaches vanishes. This observation confirms that the proposed method reaches the correct physical limit.

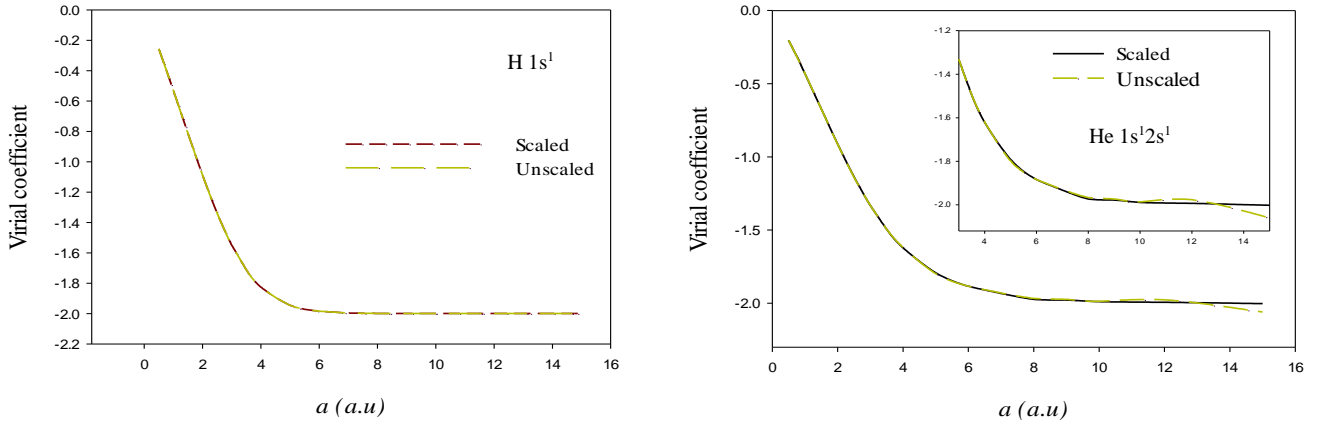


Figure 2. Virial coefficients as a function of radius for one- and two-electron quantum dot structures (H $1s^1$ and He $1s^1 2s^1$) confined by an infinite potential barrier.

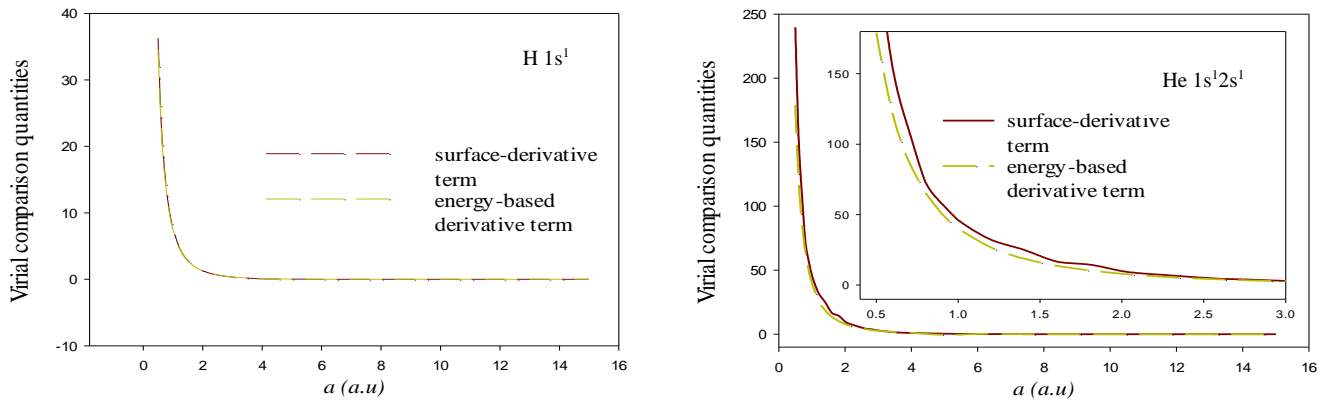


Figure 3. Radial dependence of the derivative terms appearing in the virial analysis for confined H($1s^1$) and He($1s^1 2s^1$) quantum dot systems with an infinite potential barrier. The surface-derivative term $\frac{a^3}{2} \left(\frac{dR_{n,l}}{dr} \Big|_{r=a} \right)^2$ and the energy-based derivative term $a \frac{dE(\eta,a)}{da}$ are shown for comparison.

The term $\frac{dE}{da}$ used in this study was calculated and validated through two distinct methods. First, within the QGA cycle, the energy functional is analytically derived, and the algorithm's operation is entirely founded upon this analytical $\frac{dE}{da}$ information.

After the optimization was completed, the same derivative for the final wave functions was calculated again, this time completely numerically, by applying the fourth-order five-point central difference formula and Richardson extrapolation. The analytical and numerical derivatives are in excellent agreement over the entire radius range. This consistency strongly confirms the accuracy of the derivative and the numerical stability of the scaling method.

In this study, energy components and derivative behavior of quantum dot structures (H $1s^1$ and He $1s^1 2s^1$) confined by an infinite potential barrier were examined in detail in a way that satisfies the conditions of the virial theorem. Application of the virial theorem in the energy minimization process enabled the system to reach a more consistent structure both mathematically and physically.

It was observed that the fluctuations in the drawn energy graphs decreased significantly. This is due to both

the correct control of the number of nodes and the execution of energy minimization together with the virial condition. In addition, the fact that the virial coefficients approach -2 as expected with the radius confirms that the calculations are fully compatible with the virial theorem. Analysis of the derivatives of energy functions has shown that at small radii approximate wave functions cannot fully represent the physical behavior. When the derivative values obtained via numerical methods were compared with the analytical expressions derived from the wave functions, they exhibited deviations at small radii and strong agreement at large radii. This difference shows that in bounded systems, the virial theorem may not be fully satisfied in all cases for approximate solutions, especially the boundary conditions are decisive in determining the slope behavior of the wave functions.

Our analysis reveals that the application of the virial theorem ensures the consistency and regularity of the energy components in quantum dot systems with infinite potential barriers. Furthermore, it serves as an effective tool for assessing the accuracy of approximate wave functions.

Conflict of Interest

There are no conflicts of interest in this work.

Acknowledgments

The author is grateful to Prof. Dr. Ayhan Özmen for his valuable contributions to this work.

References

- [1] Clausius, R. (1870). On a mechanical theorem applicable to heat. *The London, Edinburgh, and Dublin Philosophical Magazine and Journal of Science*, 40(265), 122–127. <https://doi.org/10.1080/14786447008640370>
- [2] Ladera, C. L., Alomá, E., & León, P. (2010). The virial theorem and its applications in the teaching of modern physics. *Latin-American Journal of Physics Education*, 4(2), 1.
- [3] Thomas, J., Kinast, J., & Turlapov, A. (2005). Virial theorem and universality in a unitary Fermi gas. *Physical Review Letters*, 95(12), 120402. <https://doi.org/10.1103/PhysRevLett.95.120402>
- [4] Peebles, P. (1976). A cosmic virial theorem. *Astrophysics and Space Science*, 45(1), 3–19. https://ui.adsabs.harvard.edu/link_gateway/1976Ap&SS..45....3P/doi:10.1007/BF00642136
- [5] Böhmer, C. G., Harko, T., & Lobo, F. S. (2008). The generalized virial theorem in $f(R)$ gravity. *Journal of Cosmology and Astroparticle Physics*, 2008(03), 024. <https://doi.org/10.1088/1475-7516/2008/03/024>
- [6] Born, M., & Jordan, P. (1925). Zur Quantenmechanik. *Zeitschrift für Physik*, 34(1), 858–888. <https://doi.org/10.1007/BF01328531>
- [7] Born, M., Heisenberg, W., & Jordan, P. (1926). Zur Quantenmechanik II. *Zeitschrift für Physik*, 35(8), 557–615. <https://doi.org/10.1007/BF01379806>
- [8] Finkelstein, B. (1928). Über den Virialsatz in der Wellenmechanik. *Zeitschrift für Physik*, 50(3), 293–294.
- [9] Fock, V. (1930). Bemerkung zum Virialsatz. *Zeitschrift für Physik*, 63(11), 855–858.
- [10] Slater, J. C. (1933). The virial and molecular structure. *The Journal of Chemical Physics*, 1(10), 687–691. https://ui.adsabs.harvard.edu/link_gateway/1933JChPh...1..687S/doi:10.1063/1.1749227
- [11] Hirschfelder, J., & Kincaid, J. (1937). Application of the virial theorem to approximate molecular and metallic eigenfunctions. *Physical Review*, 52(6), 658. <https://doi.org/10.1103/PhysRev.52.658>
- [12] Coulson, C., & Bell, R. (1945). Kinetic energy, potential energy and force in molecule formation. *Transactions of the Faraday Society*, 41, 141–149. <https://doi.org/10.1039/TF9454100141>
- [13] Löwdin, P.-O. (1959). Scaling problem, virial theorem, and connected relations in quantum mechanics. *Journal of Molecular Spectroscopy*, 3(1–6), 46–66. [https://doi.org/10.1016/0022-2852\(59\)90006-2](https://doi.org/10.1016/0022-2852(59)90006-2)
- [14] Argyres, P. N. (1967). The virial theorem for a system of interacting particles under external forces and constraints. *International Journal of Quantum Chemistry*, 1(S1), 669–675.
- [15] Fernández, F., & Castro, E. (1981). A new treatment of enclosed quantum mechanical systems. *Journal of Physics A: Mathematical and General*, 14(12), L485. <https://doi.org/10.1088/0305-4470/14/12/002>
- [16] Fernández, F. M., & Castro, E. A. (1981). The virial theorem for systems subjected to sectionally defined potentials. *The Journal of Chemical Physics*, 75(6), 2908–2913. <https://doi.org/10.1063/1.442377>
- [17] Fernández, F. M., & Castro, E. A. (1981). Hypervirial theorems and enclosed quantum-mechanical systems. *Physical Review A*, 24(5), 2344. <https://doi.org/10.1103/PhysRevA.24.2344>
- [18] Fernández, F. M., & Castro, E. A. (1981). Hypervirial analysis of enclosed quantum mechanical systems: I. Dirichlet boundary conditions. *International Journal of Quantum Chemistry*, 19(4), 521–532. <https://doi.org/10.1002/QUA.560210513>
- [19] Fernández, F. M., & Castro, E. A. (1982). Virial theorem and boundary conditions for approximate wave functions. *International Journal of Quantum Chemistry*, 21(4), 741–751. <https://doi.org/10.1002/qua.560210408>
- [20] Katriel, J., & Montgomery, H. (2012). The virial theorem for the smoothly and sharply, penetrably and impenetrably confined hydrogen atom. *The Journal of Chemical Physics*, 137(11). <https://doi.org/10.1063/1.4753424>
- [21] Mukherjee, N., & Roy, A. K. (2019). Quantum mechanical virial-like theorem for confined quantum systems. *Physical Review A*, 99(2), 022123. <https://doi.org/10.1103/PhysRevA.99.022123>
- [22] Mukhopadhyay, S., & Bhattacharyya, K. (2005). Confined systems and the modified virial theorem from semiclassical considerations. *International Journal of Quantum Chemistry*, 101(1), 27–32. <https://doi.org/10.1002/qua.20220>
- [23] Cabrera-Trujillo, R., & Vendrell, O. (2020). On the virial theorem for a particle in a box: Accounting for Cauchy's boundary condition. *American Journal of Physics*, 88(12), 1103–1108. <https://doi.org/10.1119/10.0001802>
- [24] Sezer, M. Ö. (2024). Employing virial coefficients for optimal solutions in variational calculations. *Cumhuriyet Science Journal*, 45(3), 604–608.
- [25] Demir, C., Çakır, B., Yakar, Y., & Özmen, A. (2023). Energies of the ground and excited states of confined two-electron atom in finite potential well. *Physica B: Condensed Matter*, 662, 414967. <https://doi.org/10.1016/j.physb.2023.414967>
- [26] Levine, I. N., Busch, D. H., & Shull, H. (2009). *Quantum chemistry*. Pearson Prentice Hall.
- [27] Cakir, B., Özmen, A., Atav, U., Yüksel, H. N., & Yakar, Y. (2007). Investigation of electronic structure of a quantum dot using Slater-type orbitals and quantum genetic algorithm. *International Journal of Modern Physics C*, 18(1), 61–72. <https://doi.org/10.1142/S0129183107010255>